Discussion of a *Cobalt* V9.2 Verification Case

W. Z. Strang

Cobalt Solutions, LLC. recently released *Cobalt* version V9.2. This version, as well as versions V9.0 and V9.1, makes third- and fourth-order spatial accuracies available to users. One of the primary verification cases used in the development of version V9.2 is the widely-known advecting vortex case; Pulliam [1] being one of many possible references. Results for this verification case are presented below.

Verification Case Description

A popular test case is used to assess the nominal order-of-accuracy of the reconstruction methods in *Cobalt* V9.2: an isentropic advecting vortex [1]. The non-dimensional initial conditions, using the non-dimensionalizations in *Cobalt* V9.2, for the vortex super-imposed on a uniform background flow are:

$$T = T_\infty - \frac{V_s^2(\gamma - 1)}{16 G_s \gamma \pi^2} e^{2G_s(1-r^2)}$$

$$\rho = \left(\frac{T}{S_\infty}\right)^{\frac{1}{(\gamma-1)}}$$

$$p = \rho T$$

$$u = u_\infty - \frac{V_s}{2\pi}(y - y_0) e^{G_s(1-r^2)}$$

$$v = v_\infty + \frac{V_s}{2\pi}(x - x_0) e^{G_s(1-r^2)}$$

$$S_\infty \equiv \frac{p_\infty}{\rho_\infty^\gamma}$$

$$r = \sqrt{(x - x_0)^2 + (y - y_0)^2}$$

where $\rho_\infty = 1.0;\ p_\infty = {}^{1.0}/_{\gamma}\,;\ u_\infty = 0.5;\ v_\infty = 0.0;\ T_\infty = {}^{1.0}/_{\gamma}\,;\ \gamma = 1.4,\ V_s = 5.0$, and $G_s = 0.5$. The terms V_s and G_s are the vortex strength and Gaussian width scale, respectively, and the vortex is initially centered at (x_0, y_0).

Reconstruction Tests

For the reconstruction tests, the domain is a square of size 10.0 units by 10.0 units discretized by 10, 20, 40, 80, and 160 quadrilateral (square) cells in each direction, with the edge lengths of each cell being thus 1.0, 0.5, 0.25, 0.125, and 0.0625, respectively. The vortex center (x_0, y_0) = (5.0,5.0); the initial cell-averaged values are computed using p=6 Gaussian quadrature. Data at the quadrature points of every edge are found by reconstruction and differences between the reconstructed data and the analytical values are recorded. Figure 1 plots the L_2 norm of the reconstruction error of u, the x-component of velocity. The L_∞ norm shows essentially the same behavior and is not plotted for clarity. Error norms for other variables also show the same behavior and are not shown.

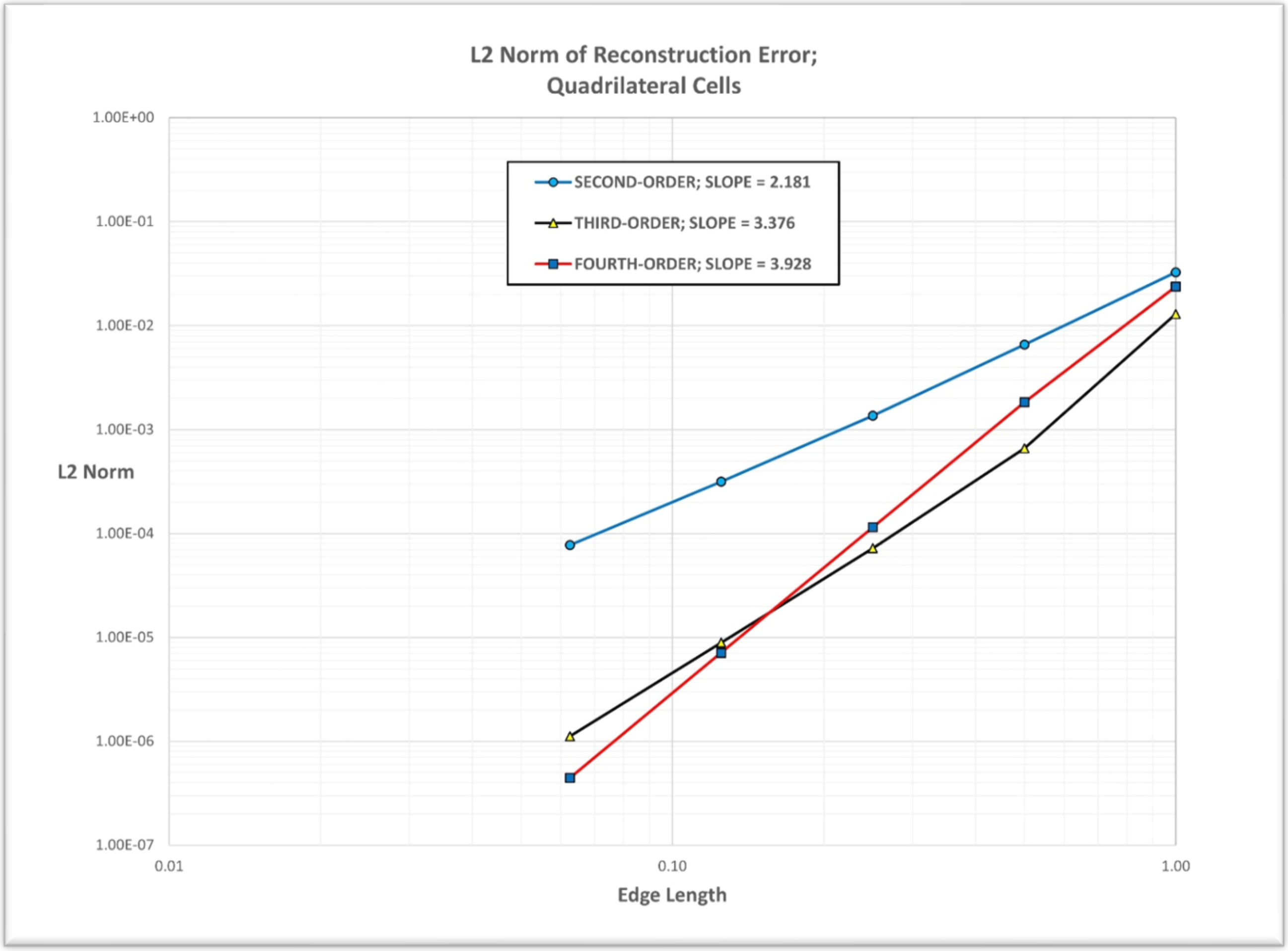

Figure 1. L2 Norm of Reconstruction Error, Quadrilateral Cells

Results over equilateral triangular grids with the same edge lengths as the quadrilateral grids are shown in Figure 2. Note that, due to the domains being tessellated with triangles, the domains are now nominally 10 by 10 units.

Square cells with edge length L have an area of L^2 and the distance between adjacent cell centroids is L. Equilateral cells with edge length L, on the other hand, have an area of $\left(\frac{\sqrt{3}}{4}\right) L^2 \cong 0.433L^2$ and the distance between adjacent cell centroids is $\frac{L}{\sqrt{3}} \cong 0.577L$. Therefore, when comparing results between equilateral grids and quadrilateral grids with equal edge lengths, the equilateral grids will behave with higher resolution in cell-centered, finite volume methods, such as *Cobalt* V9.2. This is observed in the following results.

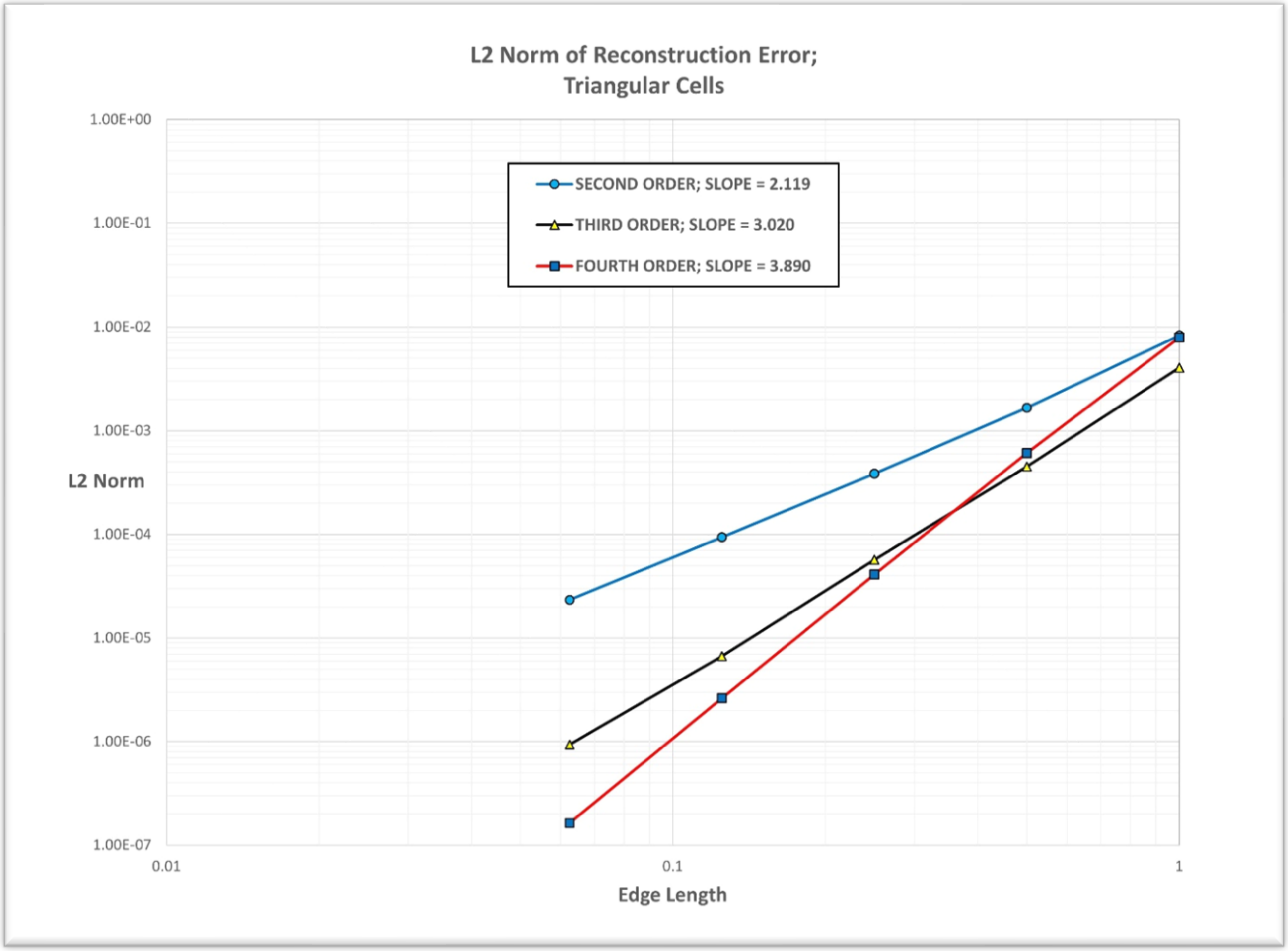

Figure 2. L2 Norm of Reconstruction Error, Triangular Cells

Orders of reconstruction accuracy are tabulated below:

Method	Quadrilateral Cells	Triangular Cells
Second Order	2.181	2.119
Third Order	3.376 - 3.070	3.020
Fourth Order	3.928	3.890

Table 1. Reconstruction Order

Note that while the slope of the k=2 reconstruction on quadrilateral cells is 3.376 over the entire range of grid spacing, it is 3.070 with the coarsest spacing omitted.

On a related note, a test polynomial data variation of the form:

$$P(x,y,z) = \alpha_1 x + \alpha_2 y + \alpha_3 z + \alpha_4 x^2 + \alpha_5 y^2 + \alpha_6 z^2 + \alpha_7 xy + \alpha_8 yz + \alpha_9 zx + \alpha_{10} x^3 + \alpha_{11} y^3 + \alpha_{12} z^3 + \alpha_{13} x^2 y + \alpha_{14} xy^2 + \alpha_{15} y^2 z + \alpha_{16} yz^2 + \alpha_{17} z^2 x + \alpha_{18} zx^2 + \alpha_{19} xyz$$

was used to verify k-exactness of the reconstructions on a wide variety of grids in addition to this one specific case. Linear, quadratic, and cubic variations in two and three dimensions are selected by suitable choice of the various α_i constants. Cell-averaged values of the test polynomial were computed and reconstructions based on these cell-average values were then performed. The L_∞norms of the differences between the reconstructed values and test polynomial values, for all derivatives from orders zero through k, at every face Gauss quadrature point in the given grid were computed. These tests were performed over many grids ranging from simple two-dimensional grids to Overset grids and complex 'real world' three-dimensional grids. The L_∞norm of the error for any derivative of order zero through k≤3 was never more than round-off for every grid investigated.

Advection Tests

This case was next simulated with *Cobalt* V9.2 on the above quadrilateral and triangular grids with one modification. For two reasons, the grids are now 70.0 units long in the x-direction and 20.0 units high in the y-direction. First, when the grid is 10.0 units high in the y-direction, the vortex on the coarsest grids, with edge length of 1.0, will smear enough to begin interacting with the upper and lower boundaries, contaminating the solution. Second, the fourth-order accurate method is only second-order accurate across periodic boundaries; it is, of course, fourth-order accurate across processor boundaries. To have consistent comparisons, all methods were therefore run on 70.0 by 20.0 grids. Periodic conditions are placed on all four boundaries.

Note that the vortex proper initially spans approximately four to five, nine, 19, 39, and 79 edge lengths on each successively finer grid.

The simulations were run second-order accurate in time to a non-dimensional time of 100. For best accuracy, the 1.0 and 0.5 edge length grids require three

Newton sub-iterations and a rather small non-dimensional time-step of 0.2. However, the 0.25, 0.125, and 0.0625 edge length grid results are essentially unchanged using two Newton sub-iterations with a time-step twice as large. To again ensure consistent comparisons, all simulations were therefore run with three Newton sub-iterations and non-dimensional time-steps of 0.2, 0.1, 0.05, 0.025, and 0.0125 for each successively finer grid.

To ease data post-processing, the initial vortex center in quadrilateral grids is now located at the centroid of the cell whose lower left vertex is (5.0,10.0). Thus, (x_0, y_0) is located at (5.5, 10.5), (5.25,10.25), and so on for each successively finer grid. The vortex center in triangular grids is initially located in the cell whose centroid is closest to (5.0, 10.0).

The initial cell-averaged values were again computed with p=6 Gaussian quadrature. At the conclusion of each simulation, the normal post-processing procedures in *Cobalt* V9.2 were circumvented. These post-processing procedures involve an inherent averaging step that adversely affects the comparisons with theory for this case. Instead, the actual cell-averaged density values for the horizontal row of cells with centroids lying along the line $y = y_0$ were directly output.

For brevity the results for the finest grids, those with 0.0625 edge length, are not presented as they show nothing new of interest.

Tabulated Minimum Non-Dimensional Densities

Minimum cell-averaged, non-dimensional densities, which occur at the vortex center, at the non-dimensional time of 100 are presented in Tables 1 and 3 below. Tables 2 and 4 present the data recast as percentage loss of amplitude in the density profile at the vortex center, defined as:

$$Loss\ \% \equiv \left(\frac{\rho_{computed} - \rho_{exact}}{1 - \rho_{exact}}\right) * 100$$

Note that dispersion errors may cause the vortex center to not fall in the cell with a centroid location of $(x_0 + 50, y_0)$, which is where the vortex center would theoretically fall at a non-dimensional time of 100.

Quadrilateral Grids

Method	L=1.0	L=0.5	L=0.25	L=0.125
Exact	0.42169789	0.36709141	0.35293415	0.34937088
2^{nd}-order	0.96588296	0.88149881	0.60677956	0.39529065
3^{rd}-order	0.90570383	0.53733345	0.35630281	0.34948736
4^{th}-order	0.94447051	0.80163704	0.38727349	0.34995254

Table 1. Minimum Non-Dimensional Density on Quadrilateral Grids

Method	L=1.0	L=0.5	L=0.25	L=0.125
2^{nd}-order	94.10%	81.28%	39.23%	7.06%
3^{rd}-order	83.69%	26.90%	0.52%	0.018%
4^{th}-order	90.40%	68.66%	5.31%	0.089%

Table 2. Amplitude Loss on Quadrilateral Grids

Triangular Grids

Method	L=1.0	L=0.5	L=0.25	L=0.125
Exact	0.38557894	0.35766603	0.35055933	0.34877614
2^{nd}-order	0.92895987	0.74909471	0.44832269	0.35747904
3^{rd}-order	0.85689929	0.40646510	0.35329233	0.34911582
4^{th}-order	0.93961885	0.44574567	0.35166469	0.34882751

Table 3. Minimum Non-Dimensional Density on Triangular Grids

Method	L=1.0	L=0.5	L=0.25	L=0.125
2^{nd}-order	88.44%	60.94%	15.05%	1.34%
3^{rd}-order	76.71%	7.60%	0.42%	0.052%
4^{th}-order	90.17%	13.71%	0.17%	0.008%

Table 4. Amplitude Loss on Triangular Grids

Centerline Plots

Figures 1 through 7, show cell-averaged, non-dimensional density profiles along the horizontal row of cells whose centroids lie along the line $y = y_0$. Dispersion errors can/will cause the plotted centerline minimum density to differ from the tabulated minimum density.

For brevity, centerline plots are not shown for the 0.125 edge length triangular grids as they show nothing that cannot be inferred from the 0.25 edge length triangular grid and 0.125 quadrilateral grid plots.

Quadrilateral Grids

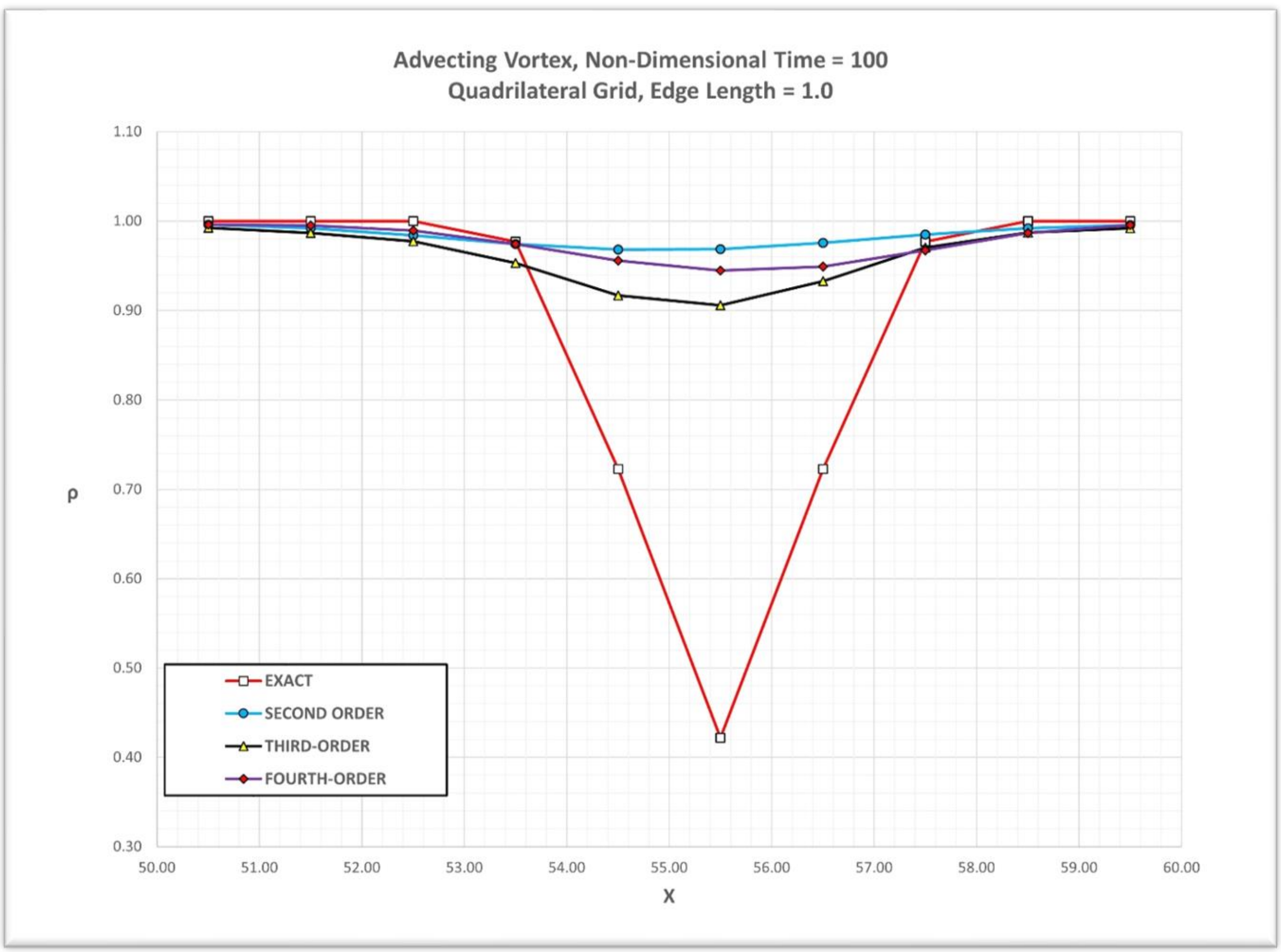

Figure 1. Edge Length = 1.0

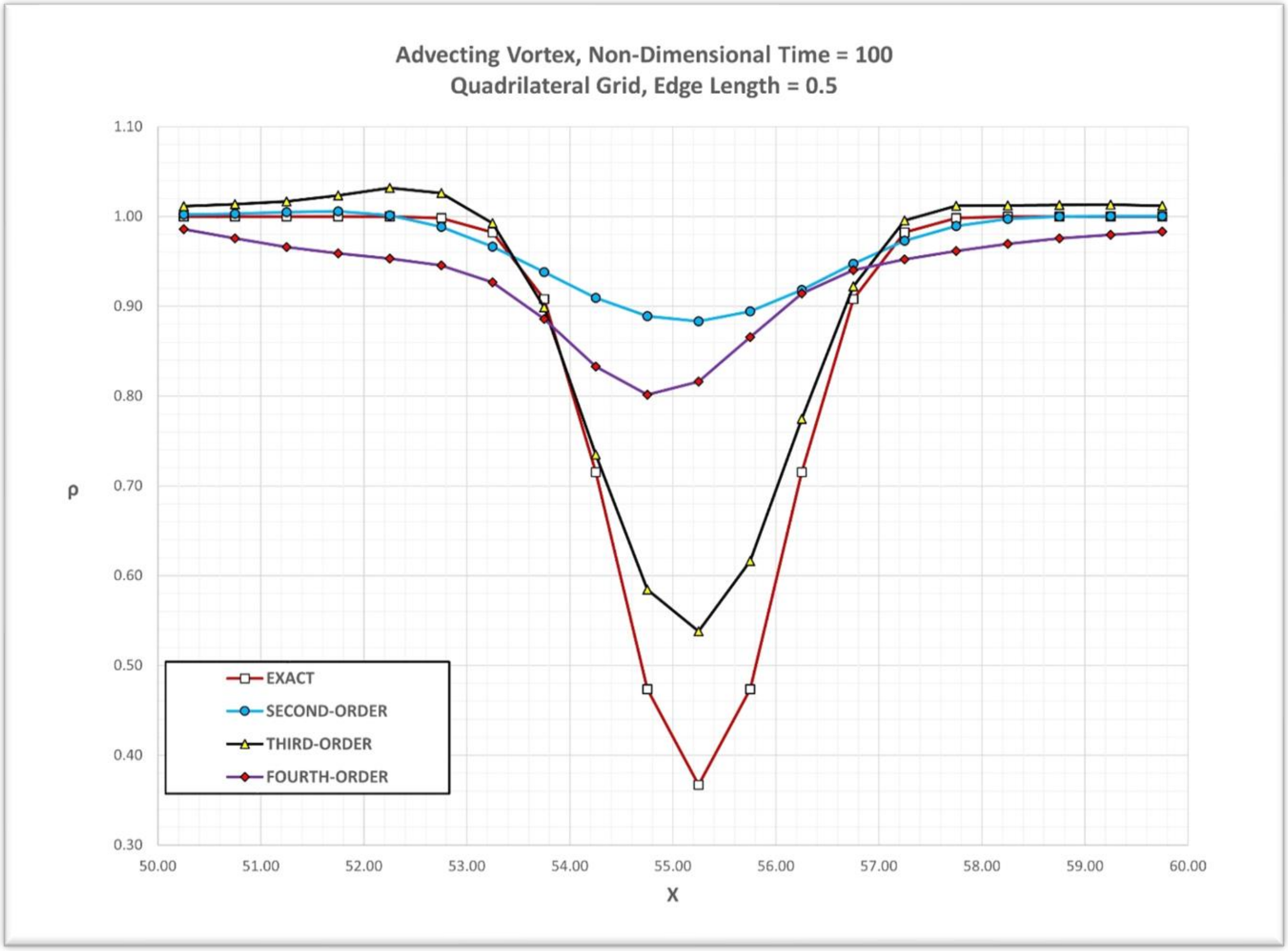

Figure 2. Edge Length = 0.5

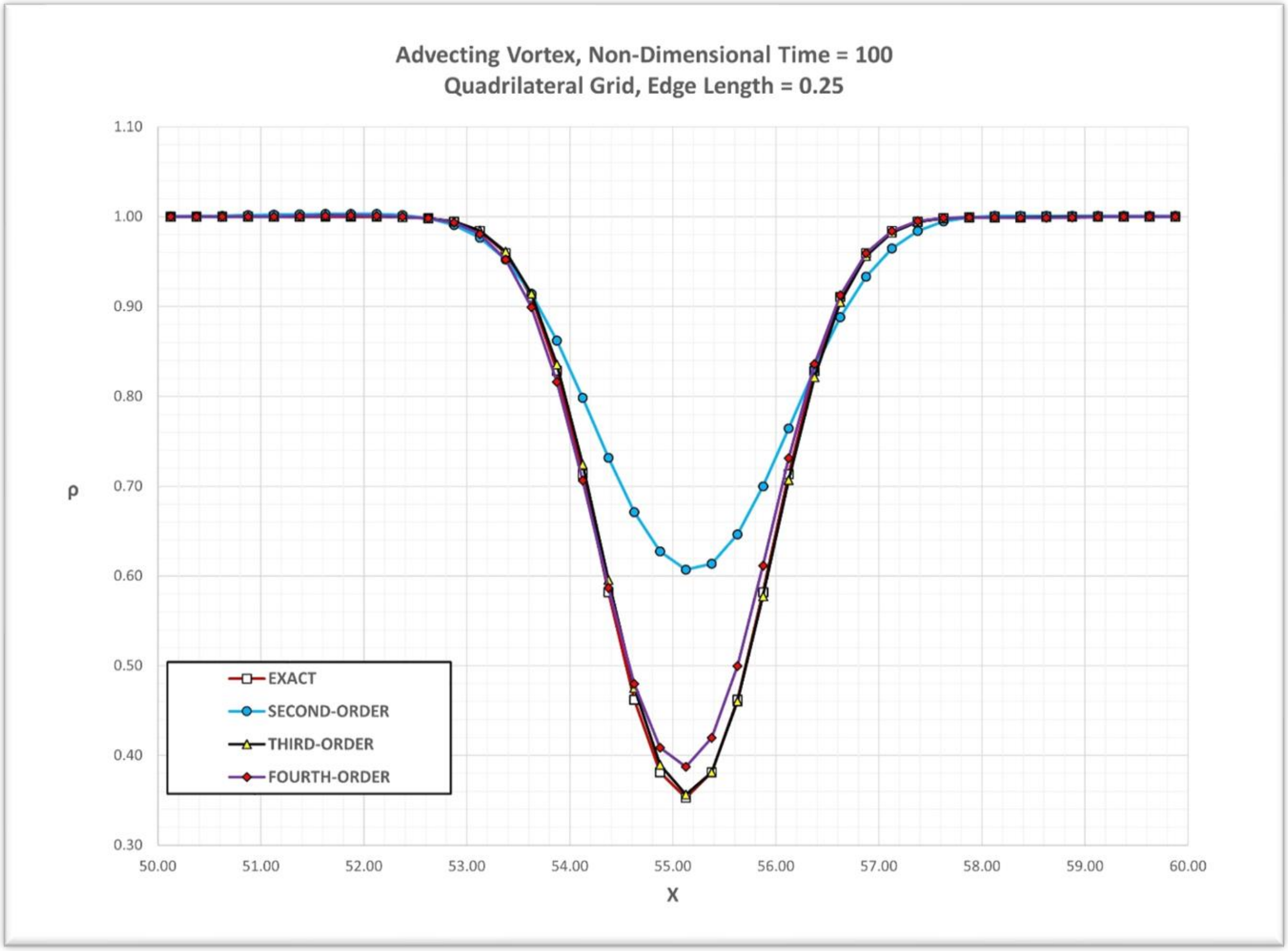

Figure 3. Edge Length = 0.25

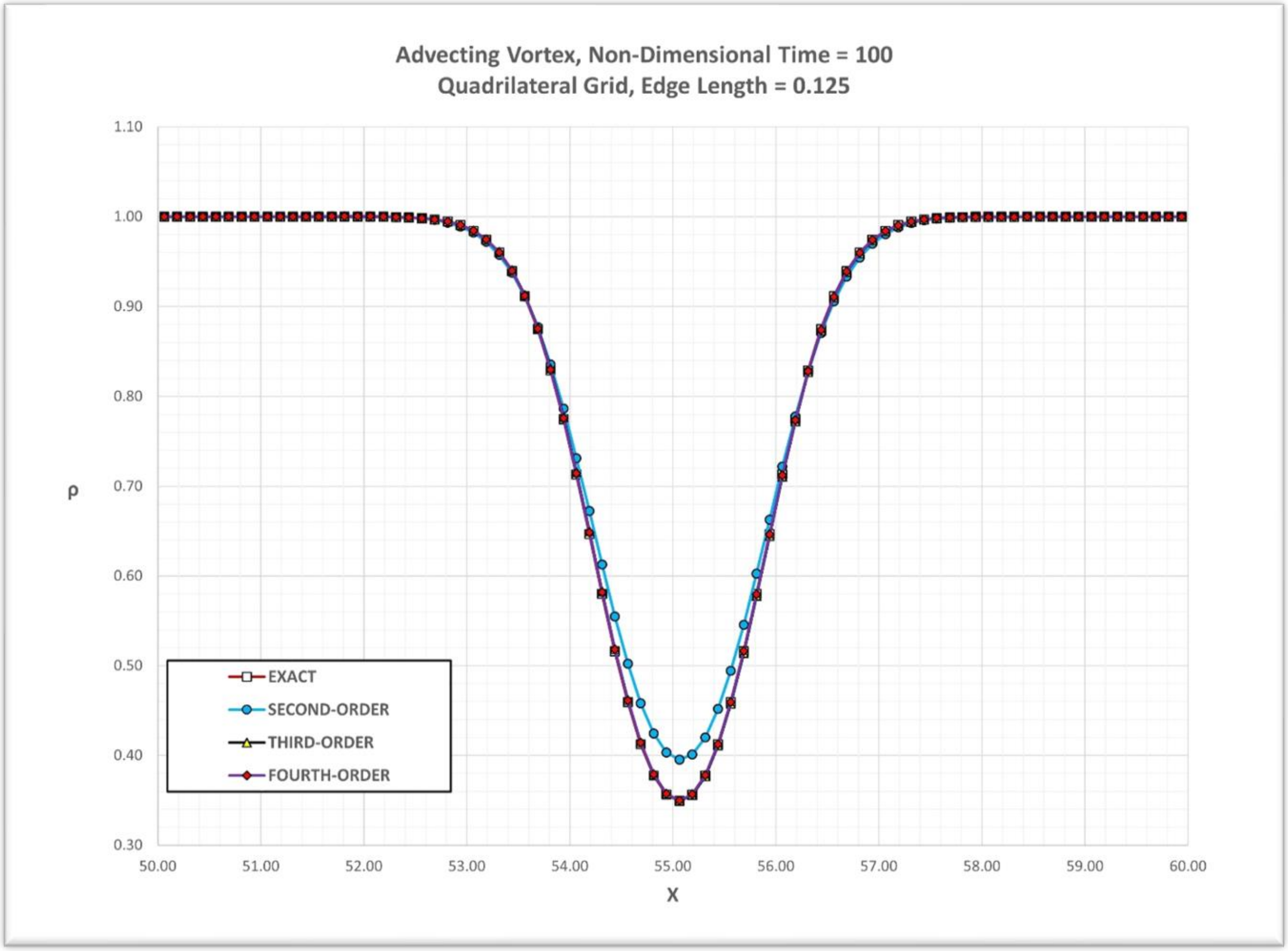

Figure 4. Edge Length = 0.125

Triangular Grids

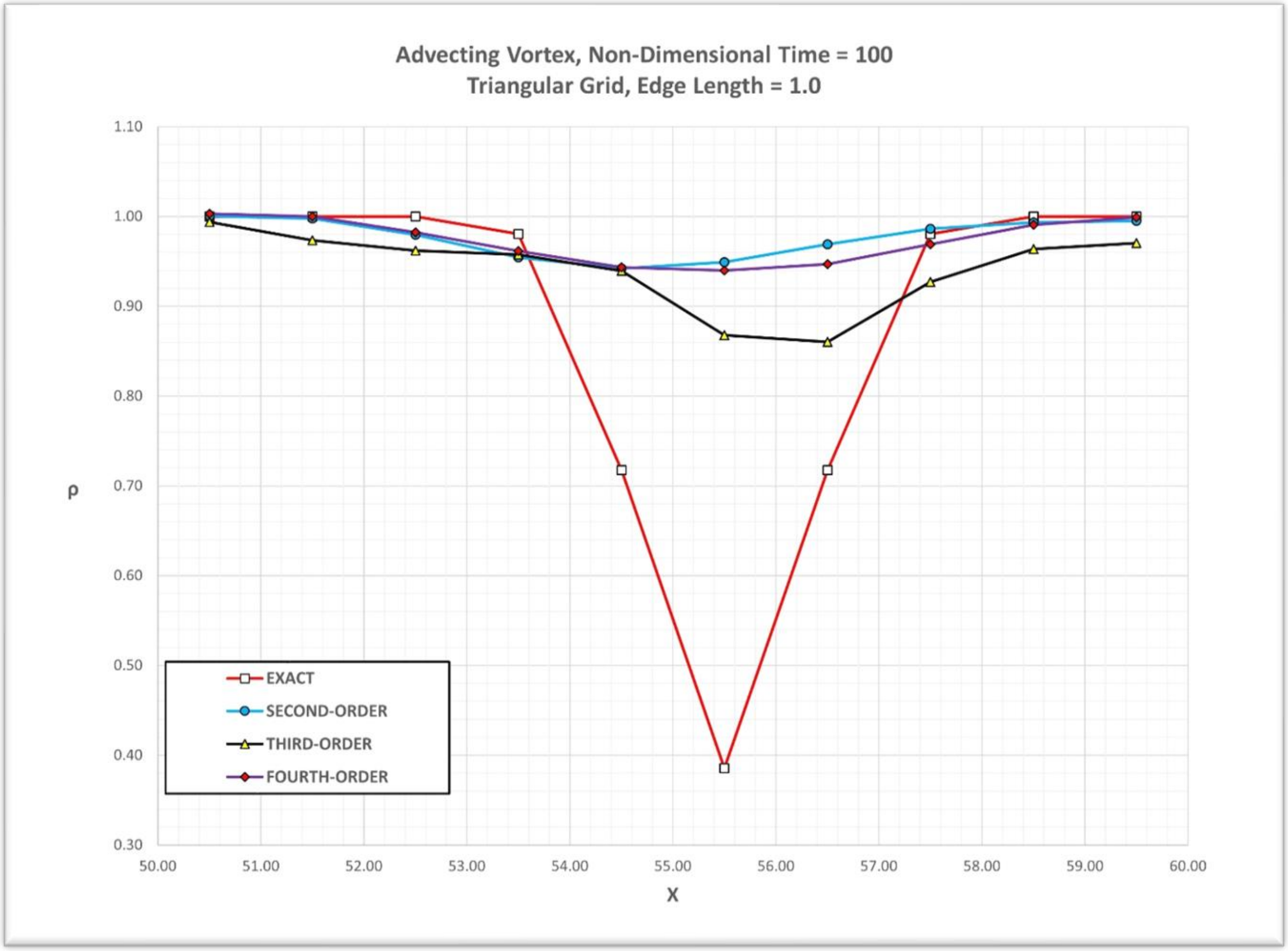

Figure 5. Edge Length = 1.0

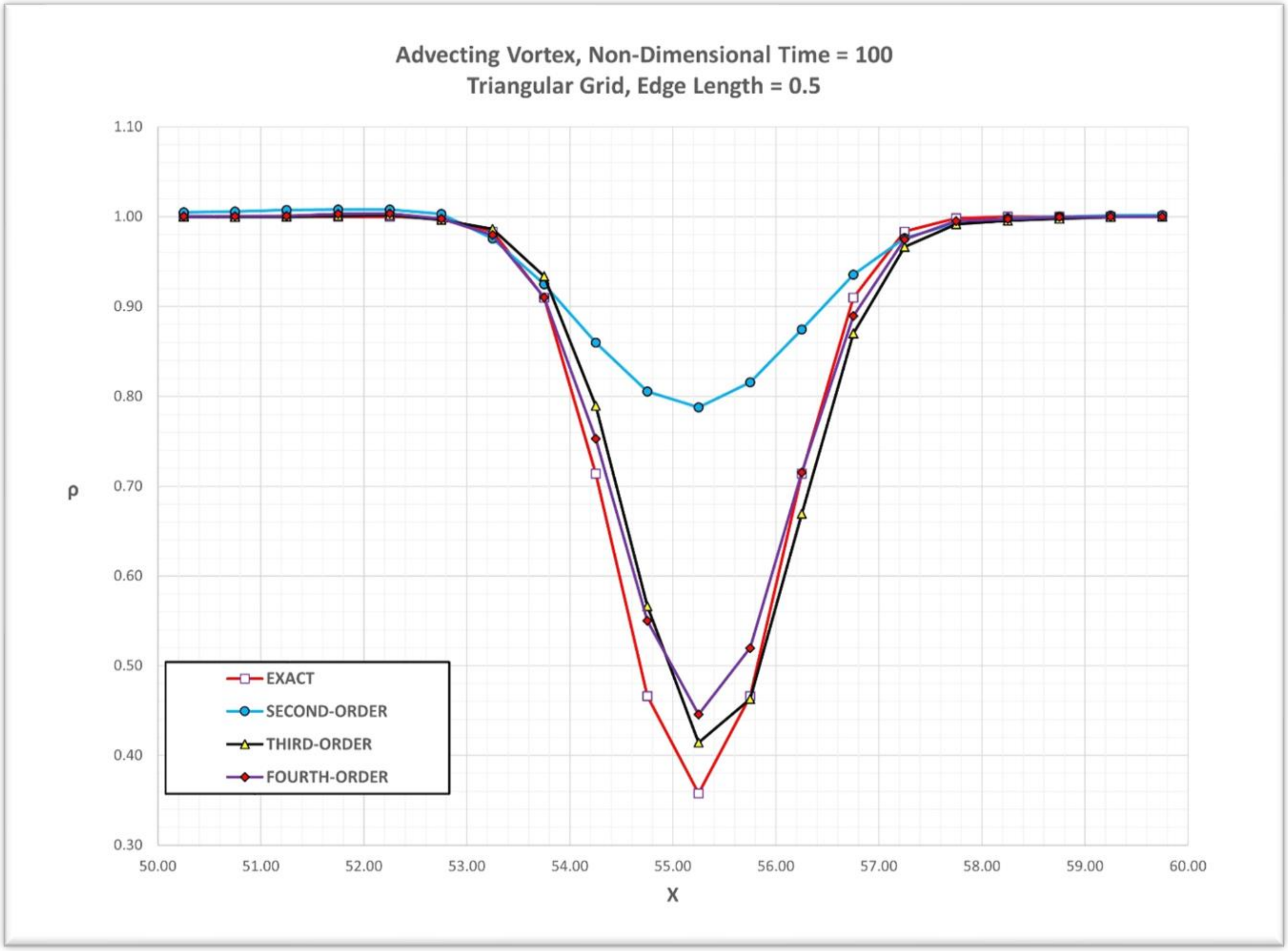

Figure 6. Edge Length = 0.5

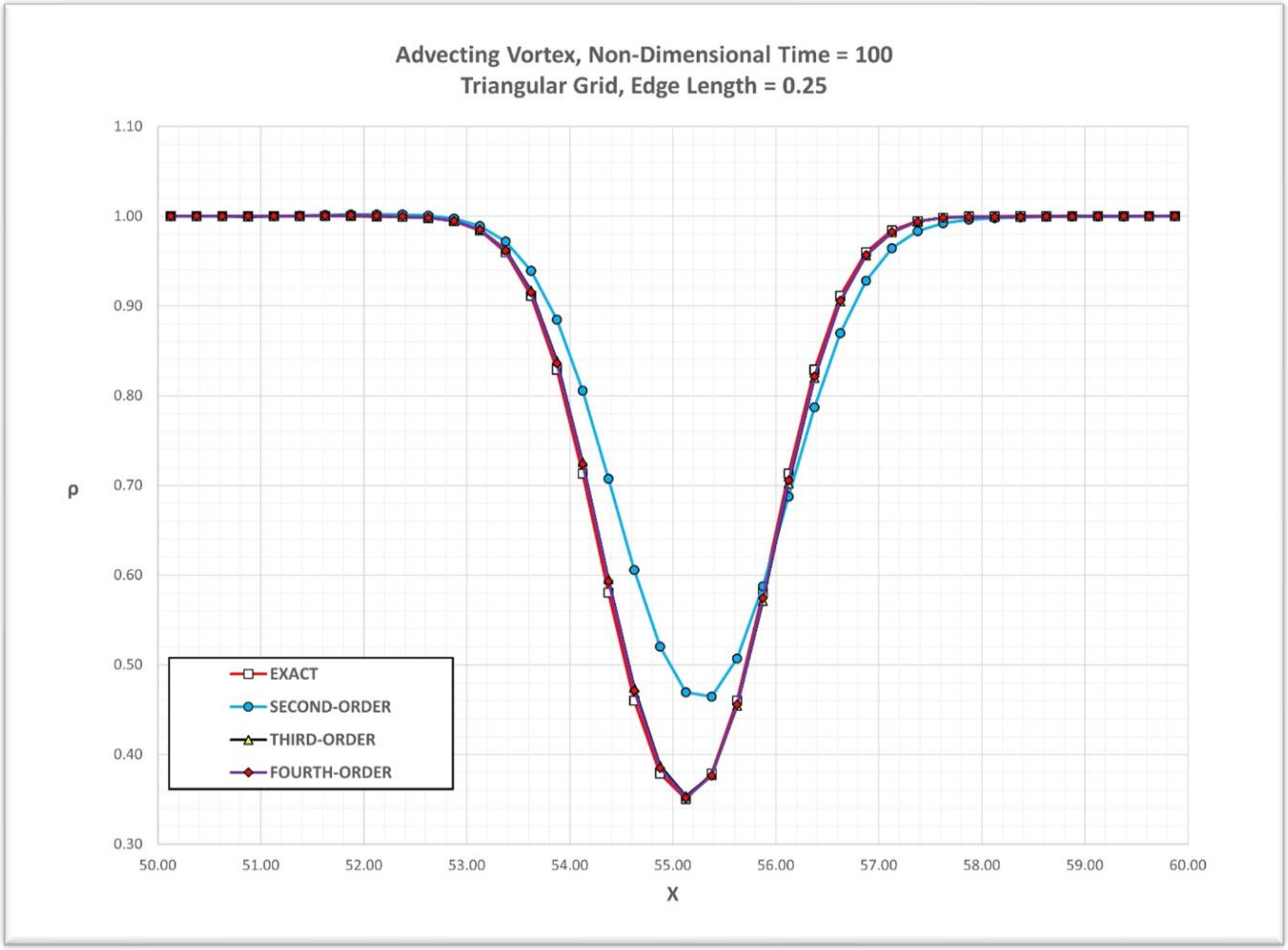

Figure 7. Edge Length = 0.25

Contour Plots

Figures 8 through 20 show contours of dimensional density for selected methods and grids. The difference between successive contour lines is ~0.02 for all figures.

For brevity, contour plots are not shown for the 0.125 edge length triangular grids as they show nothing that cannot be inferred from the 0.25 edge length triangular grid and 0.125 quadrilateral grid plots.

Quadrilateral Grids

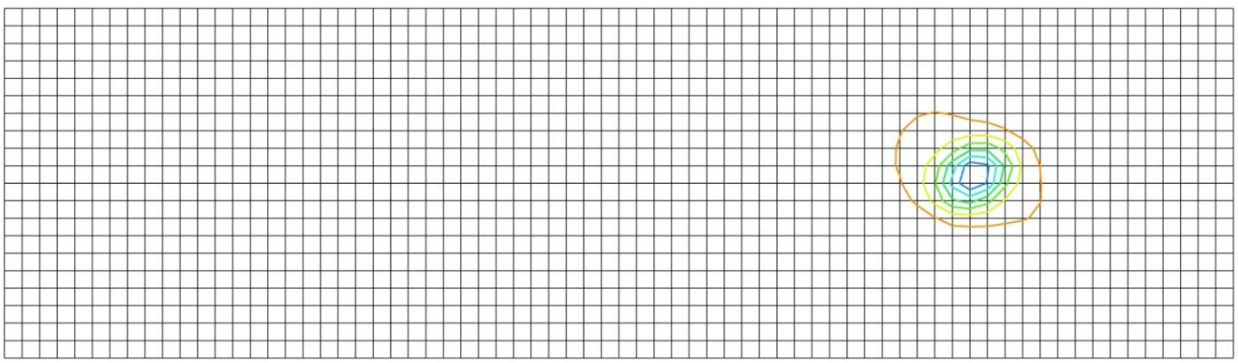

Figure 8. Edge Length = 1.0, Third-Order

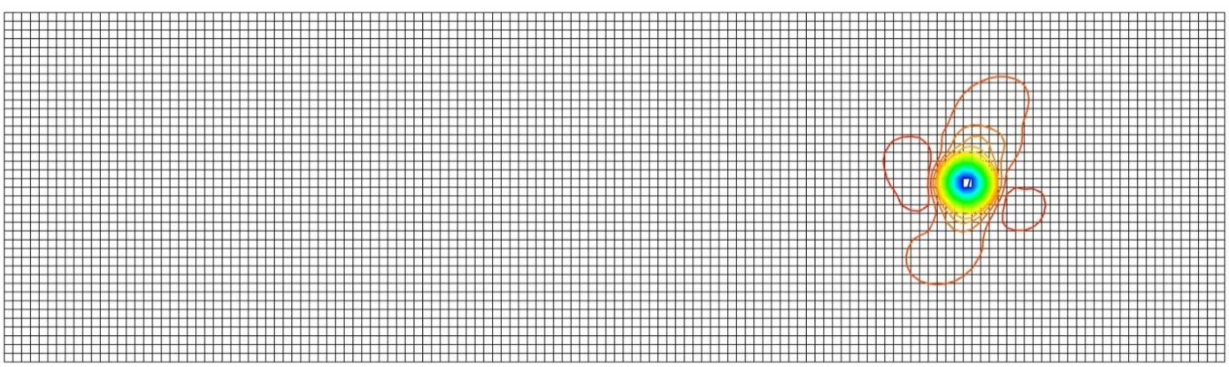

Figure 9. Edge Length = 0.5, Third-Order

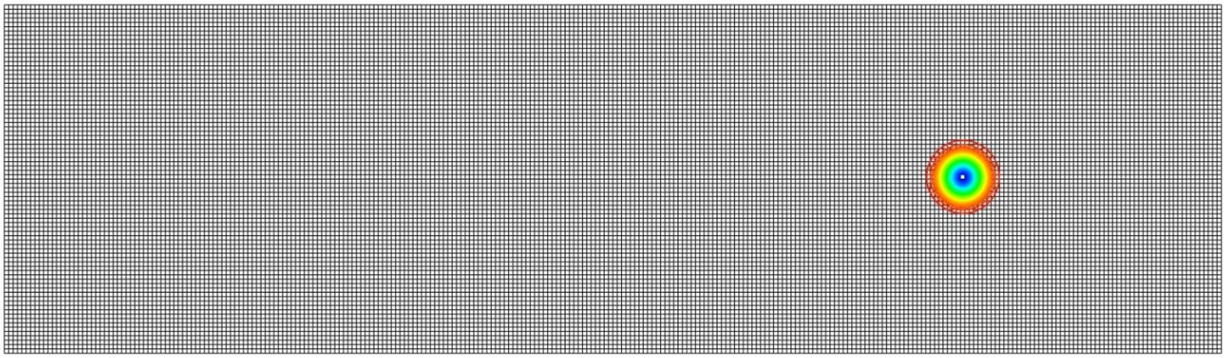

Figure 10. Edge Length = 0.25, Third-Order

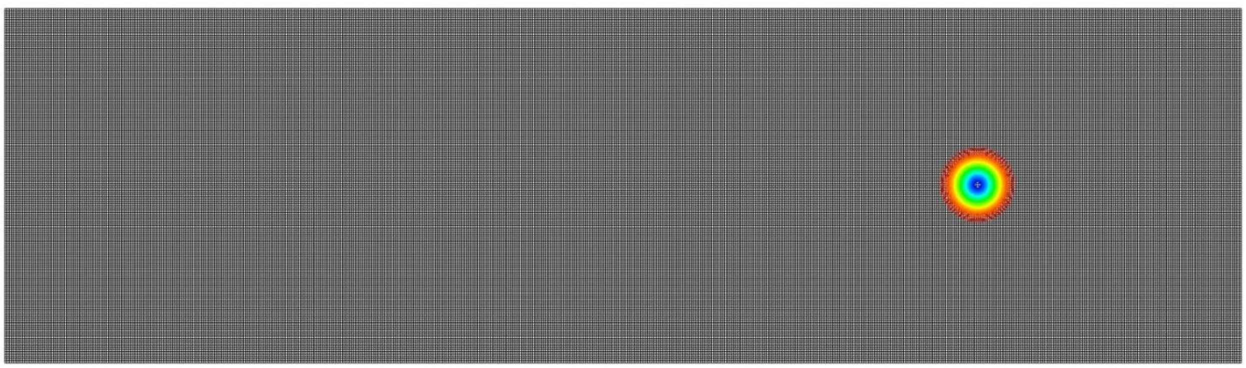

Figure 11. Edge Length = 0.125, Third-Order

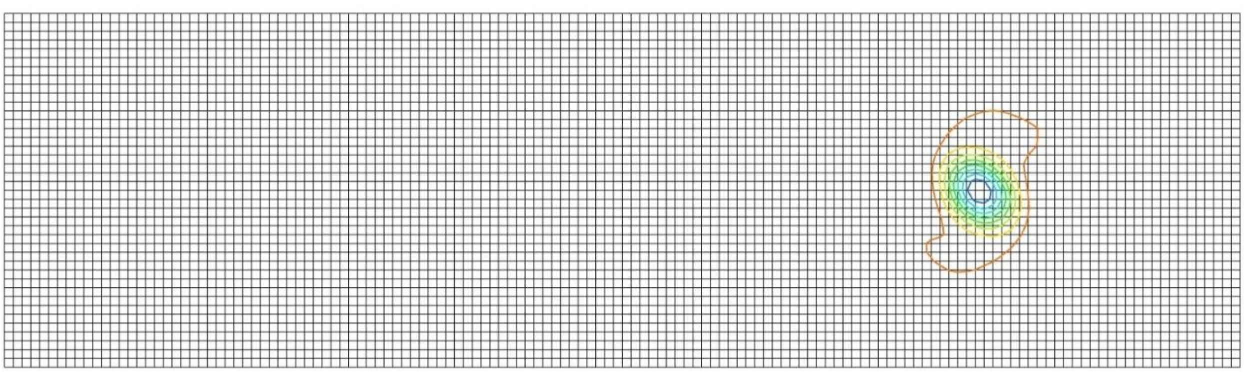

Figure 12. Edge Length = 0.5, Second-Order

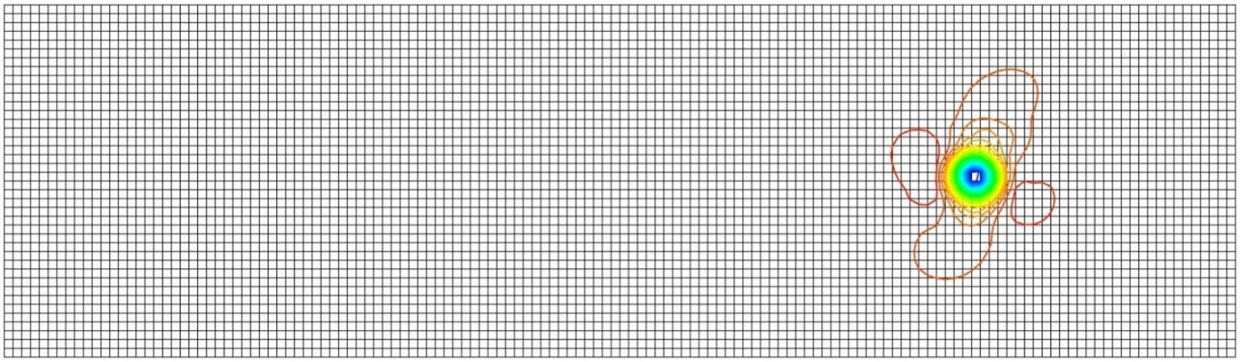

Figure 13. Edge Length = 0.5, Third-Order

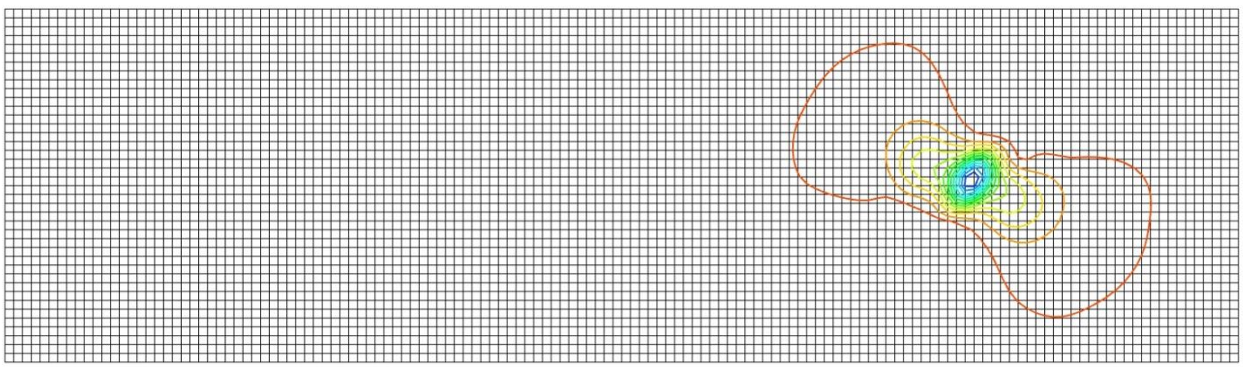

Figure 14. Edge Length = 0.5, Fourth-Order

Triangular Grids

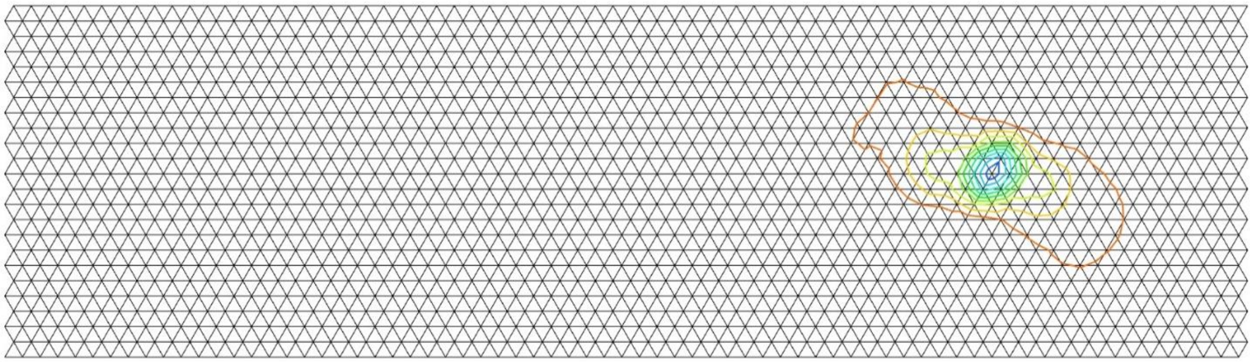

Figure 15. Edge Length =1.0, Third-Order

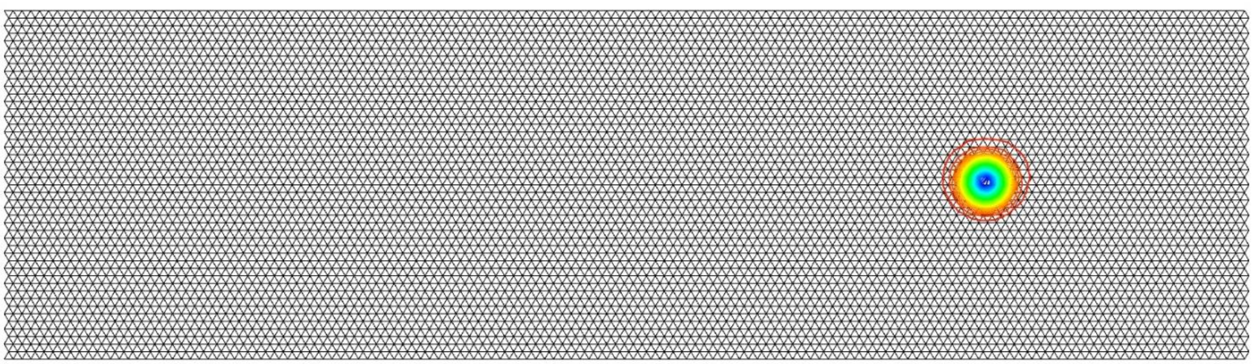

Figure 16. Edge Length = 0.5, Third-Order

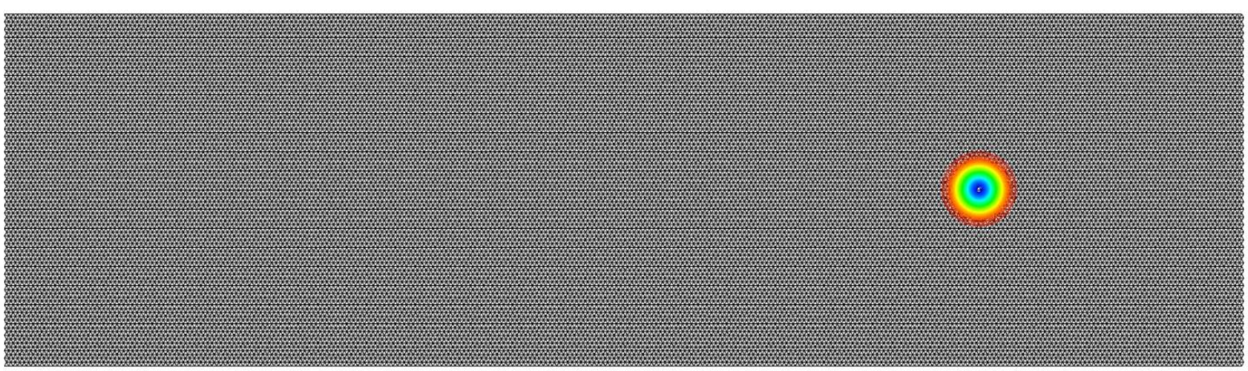

Figure 17. Edge Length = 0.25, Third-Order

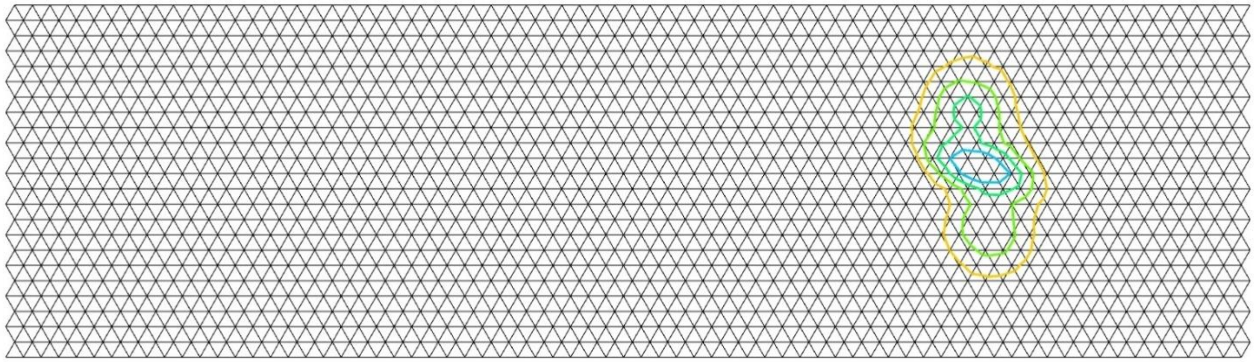

Figure 18. Edge Length = 1.0, Fourth-Order

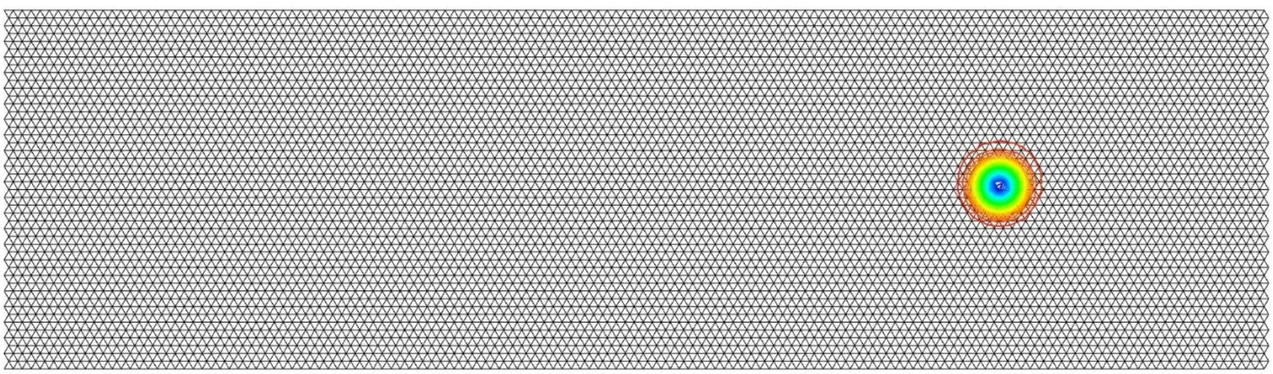

Figure 19. Edge Length = 0.5, Fourth-Order

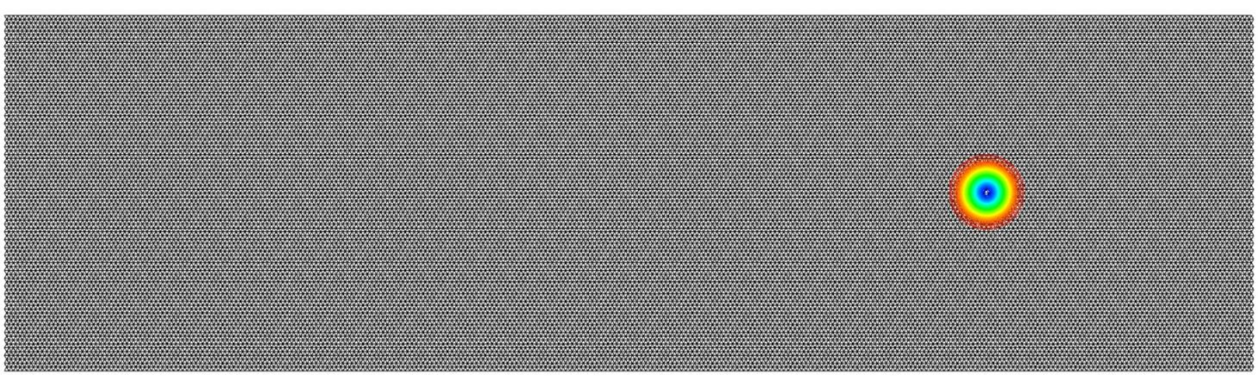

Figure 20. Edge Length = 0.25, Fourth-Order

Summary

The desired nominal orders-of-accuracy in the reconstructions are observed. Diffusion and dispersion errors are quite low for the third- and fourth-order methods once grid resolution becomes adequate. For overly coarse grids, the third- and fourth-order methods do show reduced errors compared to the second-order method, but their results are poor nonetheless. The behavior of minimum density with grid resolution does not follow nominal orders-of-accuracy due to the actions of the limiter. When activated, the limiter reduces order-of-accuracy for numerical stability.

References

1. Pulliam, T. H., “High Order Finite Difference Methods: as seen in OVERFLOW’, AIAA 2011-3851, 2011.